COLOR DECORRELATION HELPS VISUAL SALIENCY DETECTION

Boris Schauerte, Torsten Wörtwein, Rainer Stiefelhagen

Karlsruhe Institute of Technology

ABSTRACT

We present how color decorrelation allows visual saliency models to achieve higher performance when predicting where people look in images. For this purpose, we decorrelate the color information of each image, which leads to an image-specific color space with decorrelated color components. This way, we are able to improve the performance of several well-known visual saliency algorithms such as, for example, Itti and Koch's model and Hou and Zhang's spectral residual saliency. We show the advantage of color decorrelation on three eye-tracking datasets (Kootstra, Toronto, and MIT) with respect to three evaluation measures (AUC, CC, and NSS).

1 Introduction

There is evidence that specific signals in the human visual system are subject to decorrelation. For example, spatial decorrelation such as lateral inhibition operations are evident in the human vision system, which result in the visual illusion of Mach Bands [1]. Interestingly, Buchsbaum and Gottschalk [2] and Ruderman *et al*. [3] found that linear decorrelation of LMS cone responses at a point matches the opponent color coding in the human visual system. Decorrelation is beneficial, because adjacent spots in the retina will often perceive very similar values, since adjacent image regions tend to be highly correlated in intensity and color. To transmit this highly-redundant raw sensory information from the eye to the brain would be wasteful and instead the opponent color coding can be seen as a decorrelation operation that leads to a less redundant, more efficient image representation. This follows the efficient coding hypothesis of sensory coding in the brain [4], according to which the visual system should encode the information presented at the retina with as little redundancy as possible.

Many image processing algorithms, including several saliency models (*e.g*., [5]), process each image color channel separately and subsequently fuse the results. However, the color information that is encoded at each pixel is often redundant and not independent, which might lead to mishandling information that is jointly represented by the color components. For example, quaternion-based image processing tries to compensate this problem by holistically processing the color information as a whole [6], which has also been explored in the area of saliency detection in recent years [7–9]. In contrast, we suggest to decorrelate the image's color information, which can be seen as being the opposite idea to holistic color image processing. However, decorrelation has the advantage that it can serve as a preprocessing step for a wide range of existing and future algorithms, because the decorrelated color image can either serve as input image for saliency algorithms directly or its decorrelated color components can be integrated as features channels. We consider two well-known decorrelation algorithms (PCA and ZCA) and demonstrate that color decorrelation can significantly improve the ability of various visual saliency models to predict human eye fixations. To ensure meaningful evaluation results, we evaluate the effect of color decorrelation on eight saliency models over three well-known datasets with respect to three evaluation measures. This way, we show that in most scenarios color space decorrelation has a significant beneficial influence on the predictive performance of visual saliency models.

2 Related Work

Since surveying saliency models (see, *e.g*., [10]) is beyond the scope of this paper, our related work focuses on algorithms that are relevant in the remainder of this paper. Like several other traditional approaches (*e.g*., [11]), Itti and Koch's model [12] is based on feature selection, followed by center-surround operations that highlight local gradients, and a subsequent combination step that leads to the final saliency map. Harel's graph-based visual saliency [13] also follows this approach, but implements it in a graph-based model. In recent years, spectral saliency models have attracted interest (*e.g*., [5, 9, 14]) due to their performance and computational efficiency. These models manipulate the image's frequency spectrum to highlight sparse salient regions. Hou and Zhang introduced the first model, which suppresses the magnitude component in the Fourier transform's (FFT) frequency spectrum [14]. Later, Hou *et al*. proposed to use the discrete cosine transform (DCT) [5]. Guo *et al*. [7] proposed to realize Hou and Zhang's approach using the hypercomplex quaternion algebra to process the image's color information holistically. Similarly, Schauerte and Stiefelhagen implemented Hou *et al*.'s DCT-based approach with hypercomplex quaternion algebra (see [9]). To detect salient objects in images, Achanta *et al*. [15] calculated each pixel's saliency depending on the pixel's deviation from the image's mean color. Consequently, this model only considers global image properties and does not consider the local pixel neighborhood. Similarly, Lu and Lim [16] calculate and invert the image's color histogram to calculate the saliency model.

Decorrelation of color information has been applied in several areas such as, *e.g.*, color enhancement [17] and color transfer [18]. More importantly, it is highly related to the human visual system and techniques such as the zero-phase transform (ZCA) have been developed and proposed to model aspects of the human visual system [19]. Buchsbaum and Gottschalk [2] and Ruderman *et al.* [3] found that linear decorrelation of LMS cone responses at a point matches the opponent color coding in the human visual system. However, when modeling the human visual system it is mostly applied in the context of spatio-chromatic decorrelation, *i.e.* local (center-surround) contrast filter operations [3, 19, 20]. Most related to our approach is Ruderman *et al.*'s color space [3], which has been calculated on a fixed image set on the basis of a logarithmic LMS color space with zero mean. Since decorrelation is an important aspect of the human visual system, it has also been part of visual saliency models. Duan *et al.* [21] explored the use of PCA on an image patch level, which is closely related Zhou *et al.*'s approach [22] in which the image is first segmented into patches and then the PCA is used to reduce the patch dimensions to throw out dimensions that are basically noise for the saliency calculation. Similarly, Wu *et al.* [23] propose to use the PCA to attenuate noise as well as to reduce computational complexity and translation errors. Luo *et al.* [24] also use the PCA on a block-wise level to differentiate between salient objects and background.

3 Image Color Decorrelation

Let $I \in \mathbf{R}^{M \times N \times K}$ be the matrix that represents an image in a color space with K components. Reshaping the image matrix and subtracting the mean color, we represent the image's mean centered color information in a color matrix $X \in \mathbf{R}^{MN \times K}$.

In general, a matrix W is a decorrelation matrix, if the covariance matrix of the transformed output $Y = XW$ satisfies

$$YY^T = \text{diagonal matrix} \quad . \tag{1}$$

In general, there will be many decorrelation matrices W that satisfy Eq. 1 and decorrelate [19]. The most common approach to decorrelation and whitening is to diagonalize the empirical sample covariance matrix

$$C' = WCW^{\mathrm{T}} = I \quad , \tag{2}$$

where C is the color covariance matrix

$$C = \frac{1}{MN} \sum_{i=1}^{MN} x_i {x_i}^T \text{ with } X = \begin{pmatrix} x_1 \\ \cdots \\ x_{MN} \end{pmatrix} \quad . \tag{3}$$

Here, C' is the covariance of Y of the data after the whitening transform $Y = XW$. However, there are multiple solutions for W. For example, the principal components analysis (PCA) computes the projection according to

$$W_{\mathrm{PCA}} = \Sigma^{-1/2} U^T \quad , \tag{4}$$

whereas the zero-phase whitening transform (ZCA) [19] calculates W according to the symmetrical solution

$$W_{\mathrm{ZCA}} = U \Sigma^{-1/2} U^T \quad . \tag{5}$$

Here, the eigenvectors of the covariance matrix are the columns of Σ and U is the diagonal matrix of eigenvalues. The dimensionality preserving color space transform is given by $Y = XW$ and results in the so-called score matrix Y that represents the projection of the image.

We reshape the score matrix Y so that it spatially corresponds with the original image and this way obtain our decorrelated color image representation $I_{\mathrm{PCA}} \in \mathbf{R}^{M \times N \times K}$. Finally, we normalize each color channel's value range to the unit interval $[0, 1]$. Although not necessary for all saliency algorithms, it is a beneficial step for algorithms that are sensitive to range differences between color components such as, *e.g.*, Achanta's frequency-tuned algorithm [15]. We can then use the decorrelated image channels as a foundation – *i.e.*, in the sense of raw input, feature, or conspicuity maps – for a wide range of visual saliency algorithms, see Sec. 4.1.

4 Evaluation

4.1 Visual Saliency Algorithms

We adapted the code of the following visual saliency algorithms – which we presented in detail in Sec. 2 – to evaluate the effect of color decorrelation: 1.) Models that rely on center-surround contrast: Itti and Koch's model (IK; [12]) and Harel's graph-based visual saliency (GBVS; [13]). 2.) Models that manipulate the image's frequency spectrum: The pure Fourier transform (PFT; [14]), DCT image signatures (DCT; [5]), quaternion-based DCT image signatures (QDCT) and eigenangle/-axis quaternion Fourier transform (EPQFT; [9]). 3.) Models that rely on global image properties and do not consider the local pixel neighborhood: Achanta *et al.*'s (AC; [15]) method and Lu and Lim's algorithm (CCH; [16]).

4.2 Datasets

Since an evaluation on a single dataset is almost always subject to dataset biases, we use three eye-tracking datasets: First, Bruce and Tsotsos's dataset ("Toronto"; [25]; 120 images that depict indoor and outdoor scenes; 20 subjects). Second, Judd *et al.*'s dataset ("MIT"; [26]; 1003 images (selected from Flickr and LabelMe; 15 subjects). Third, Kootstra *et al.*'s dataset ("Kootstra"; [27]; 100 images collected from the McGill calibrated color image database; 31 subjects).

4.3 Measures

Not unlike datasets, evaluation measures often exhibhit specific biases and characteristics. Riche *et al.* [28] group saliency evaluation measures into three classes: First, value-based metrics such as, *e.g.*, normalized scanpath saliency [11]. Second, metrics that rely on the area under the receiver operating characteristic curve (*e.g.*, [10, 26]), which fall into the group of

Method	RGB raw	RGB PCA	RGB ZCA	ICOPP raw	ICOPP PCA	ICOPP ZCA	CIE Lab raw	CIE Lab PCA	CIE Lab ZCA	RGB:PCA* raw	RGB:PCA* PCA	RGB:PCA* ZCA
NSS												
Toronto	0.9058	1.1536	1.1562	1.0869	1.1456	1.1606	1.1045	1.1687	1.1922	1.0955	1.1541	1.1559
Kootstra	0.4429	0.5221	0.5349	0.4882	0.5227	0.5269	0.4911	0.5188	0.5237	0.4874	0.5217	0.5279
MIT	0.7492	0.8647	0.8779	0.8290	0.8634	0.8627	0.8434	0.8677	0.8678	0.8281	0.8648	0.8641
CC												
Toronto	0.2671	0.3414	0.3430	0.3221	0.3392	0.3437	0.3264	0.3458	0.3528	0.3241	0.3416	0.3420
Kootstra	0.2064	0.2365	0.2397	0.2229	0.2363	0.2376	0.2242	0.2354	0.2248	0.2233	0.2363	0.2385
MIT	0.1862	0.2147	0.2178	0.2057	0.2143	0.2141	0.2096	0.2155	0.2155	0.2058	0.2148	0.2156
ROC AUC												
Toronto	0.6551	0.6834	0.6837	0.6734	0.6819	0.6848	0.6760	0.6858	0.6891	0.6754	0.6834	0.6840
Kootstra	0.5791	0.5979	0.6012	0.5922	0.5972	0.5995	0.5920	0.5967	0.5989	0.5908	0.5979	0.5991
MIT	0.6236	0.6451	0.6457	0.6374	0.6440	0.6457	0.6404	0.6460	0.6472	0.6373	0.6452	0.6452

Table 1. Mean performance as measured by NSS (top), CC (middle), and ROC AUC (bottom). As can be seen, the mean performance based on the image-dependent decorrelated color space (*i.e.*, PCA and ZCA) is always better.

location-based metrics. Third, distribution-based metrics such as, *e.g.*, the correlation coefficient [29]. We rely on three measures in our evaluation: The area under the receiver operator characteristic curve (ROC AUC), the linear correlation coefficient (CC), and the normalized scanpath saliency (NSS).

4.4 Results

Due to space limitations, we can only present the mean performance over all evaluated visual saliency algorithms for each dataset in Tab. 1. Also, we can only present the results for RGB, intensity and color opponents (ICOPP), CIE Lab, and RGB:PCA* as base color spaces. Additional tables with the performance for all eight saliency algorithms and fourteen color spaces are available at `http://bit.ly/1E3szPY`.

Here, "RGB:PCA*" is a color space that we constructed with a "PCA" based on "RGB" over all images in the McGill dataset. Thus, similar to, *e.g.*, the Ruderman color space [3], RGB:PCA* is an image-independent color space that is highly decorrelated by design (see [18]). And, interestingly, image-dependent decorrelation can significantly improve the results even for such color spaces that exhibit a low correlation by design (*e.g.*, RGB:PCA* and Lab) and not just for color spaces that are highly correlated (*e.g.*, RGB).

Since the performance differences are relatively small – which is also caused by the value range of the evaluation measures –, we want to ascertain that the results are relevant. For this purpose, we perform statistical significance tests. Therefore, we saved each evaluation metric's score for every image and algorithm. This way, we can use pairwise, two-sample t-tests to test three hypotheses: We can test whether the observed scores come from distributions with different means (*i.e.*, "means are not equal"). Then, we can test whether or not the mean achieved with the raw base color space without decorrelation is greater than the mean of the scores with the decorrelated color space (right-tailed test and left-tailed test, respectively). We perform all significance tests at a confidence level of 95%. Relying on rejected hypotheses and combining the outcomes of the tests, we have statistically strong indicators that decorrelation improved the performance (">"; *i.e.*, equal and worse means rejected), has at least equal performance (">="; *i.e.*, worse means rejected), probably has an equal performance ("="; *i.e.*, no hypothesis could be rejected), has equal or lower performance ("<="; *i.e.* better means rejected), or has lower performance ("<"; *i.e.* better and equal means rejected).

In total, we evaluated 672 configurations (14 color spaces $\times$ 8 saliency algorithms $\times$ 3 datasets$\times$ 2 decorrelation methods) with 3 evaluation measures. As can be seen in Tab. 2, color space decorrelation leads to significantly improved results in 640, 540, and 662 configurations as measured with NSS, CC, and ROC AUC, respectively. In our opinion, these benefits drastically outweigh the 15 of 2016 cases in which the performance is potentially lower (*i.e.*, "<=" or "<").

Measure	>	>=	=	<=	<
NSS	640	2	16	1	13
CC	540	27	105	0	0
ROC AUC	662	2	7	1	0

Table 2. Evaluation summary

4.5 Discussion

Let us now investigate aspects of color decorrelation and how it can help computational saliency detection. Therefore, we examine the intra and inter color component correlation of the color spaces, which is shown for some exemplarily color spaces in Tab. 3. Here, the intra color component correlation (ICCC) is the correlation of each color space's individual components (*e.g.*, the correlation the Lab color space's L and a, L and b, or a and b channels). The inter color component correlation refers to the correlation of the channels of different color spaces (*e.g.*, RGB's R channel and Lab a channel).

Does decorrelation depend on the input space? First of all, the decorrelated color space is not independent from its base color space. This comes at no surprise, because – for example – an antecedent non-linear transformation such as a conversion from RGB to Lab can naturally lead to a different

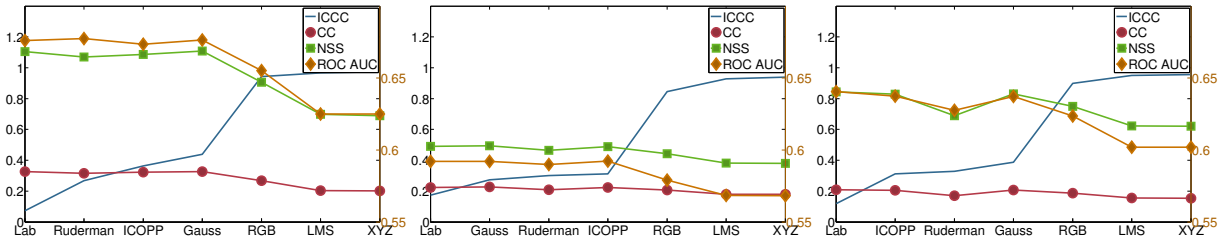

(a) Toronto (b) Kootstra (c) MIT

Fig. 1. The average performance of the evaluated visual saliency algorithms and the intra color component correlation (ICCC) for several color spaces. Left-hand scale: ICCC, CC, and NSS. Right-hand scale: ROC AUC.

		RGB			RGB:PCA*			RGB:PCA		
		1st	2nd	3rd	1st	2nd	3rd	1st	2nd	3rd
RGB	1st	1.00	0.88	0.79	0.94	0.39	0.02	0.88	0.05	0.02
RGB	2nd	0.88	1.00	0.89	0.97	0.11	0.30	0.91	0.00	0.03
RGB	3rd	0.79	0.89	1.00	0.93	0.13	0.02	0.89	0.04	0.06
Lab	1st	0.95	0.98	0.88	0.99	0.21	0.20	0.92	0.02	0.02
Lab	2nd	0.32	0.06	0.01	0.10	0.60	0.73	0.08	0.01	0.07
Lab	3rd	0.24	0.09	0.25	0.04	0.87	0.34	0.01	0.11	0.24
RGB:PCA*	1st	0.94	0.97	0.93	1.00	0.15	0.12	0.93	0.00	0.00
RGB:PCA*	2nd	0.39	0.11	0.13	0.15	1.00	0.04	0.11	0.18	0.13
RGB:PCA*	3rd	0.02	0.30	0.02	0.12	0.04	1.00	0.11	0.04	0.31
RGB:PCA	1st	0.88	0.91	0.89	0.93	0.11	0.11	1.00	0.00	0.00
RGB:PCA	2nd	0.05	0.00	0.04	0.00	0.18	0.04	0.00	1.00	0.00
RGB:PCA	3rd	0.02	0.03	0.06	0.00	0.13	0.31	0.00	0.00	1.00
Lab:PCA	1st	0.21	0.27	0.36	0.28	0.28	0.05	0.32	0.02	0.02
Lab:PCA	2nd	0.07	0.05	0.01	0.05	0.15	0.04	0.01	0.21	0.04
Lab:PCA	3rd	0.04	0.00	0.02	0.02	0.10	0.16	0.01	0.05	0.00
RGB:ZCA	1st	0.79	0.50	0.40	0.60	0.74	0.30	0.55	0.11	0.06
RGB:ZCA	2nd	0.45	0.70	0.47	0.57	0.00	0.82	0.53	0.00	0.27
RGB:ZCA	3rd	0.36	0.47	0.76	0.55	0.54	0.31	0.52	0.11	0.34

Table 3. Mean correlation strength (*i.e.*, absolute correlation value) of color space components calculated over all images in the McGill image database [30].

linear decorrelation result, which is visible by the low inter component correlation of RGB:PCA and Lab:PCA in Tab. 3. As a result, we have to neglect the notion of a base color space independent unique or shared decorrelated color projection.

Are PCA and ZCA different? The inter color component correlation between RGB:ZCA and RGB or RGB:ZCA and RGB:PCA (see Tab. 3) tell us that ZCA color projections differ substantially from PCA projections, because the ZCA does not separate luminance and chrominance information. This is of interest, because it indicates that not the separation of color and luminance itself is the key to improve the performance, but the properties of decorrelated color information.

What is the effect of decorrelation? In fact, there are two aspects of color decorrelation that can influence saliency detection: First, the color information contained in the channels is as decorrelated and thus independent as possible. This naturally supports algorithms that process the color channels independently such as, *e.g.*, DCT. Second, algorithms that use color distances (*e.g.*, AC) benefit from the aspect that color decorrelation can enhance the contrast of highly correlated images, which is the foundation of the well-known decorrelation stretch color enhancement algorithm (see [17]). In case of the PCA, this is due to the fact that the stretched (please recall that we perform a range normalization for all color spaces, see Sec. 3) and thus expanded color point cloud in the decorrelated space is less dense and spread more evenly over a wider volume of the available color space (see, *e.g.*, [17, Fig. 2]).

Can intra color component correlation (ICCC) be linked to visual saliency algorithm performance? Image-specific color decorrelation forms an extreme case of a decorrelated color space (*i.e.*, the ICCC is zero) for which we have demonstrated that it can significantly increase the performance with respect to its base color space. Since it has been noted by several authors that the color space choice influences the performance of saliency algorithms (see, *e.g.*, [5, 9]), it is interesting to investigate whether the performance differences are related to the ICCC of different color spaces. Thus, we calculated the mean performance over all evaluated visual saliency algorithms and the mean ICCC for a wider range of color spaces, see Fig. 1. As we can see, there is a relation between the average saliency detection performance and the underlying color space, which we can quantify by calculating the correlation between the ICCC and the mean saliency detection performance. These correlations are $(-0.879, -0.890, -0.893)$, $(-0.963, -0.897, -0.926)$, and $(-0.878, -0.782, -0.786)$ for (AUC, CC, NSS) on the Toronto, Kootstra, and MIT dataset, respectively. Accordingly, a high intra color component coefficient can be related to a low visual saliency detection performance on all three datasets.

5 Conclusion

We demonstrated that an image-dependent decorrelated color space can be a powerful basis for visual saliency algorithms. We evaluated the influence of decorrelated color spaces on eight saliency algorithms, which lead to significant performance improvements on three eye-tracking datasets with respect to three evaluation measures. Since the saliency algorithms that we chose to evaluate rely on three different saliency detection principles, we are confident that a wide range of other algorithms will benefit as well.

6 References

[1] F. Ratliff, *Mach Bands: Quantitative Studies on Neural Networks in the Retina*, Holden-Day, San Francisco, 1965.

[2] G. Buchsbaum and A. Gottschalk, "Trichromacy, opponent colours coding and optimum colour information transmission in the retina," *Proceedings of the Royal Society*, vol. B, no. 220, pp. 89–113, 1983.

[3] D. Ruderman, T. Cronin, and C. Chiao, "Statistics of cone responses to natural images: Implications for visual coding," *Journal of the Optical Society of America*, vol. 15, no. 8, pp. 2036–2045, 1998.

[4] H. Barlow, "Possible principles underlying the transformation of sensory messages," *Sensory Communication*, pp. 217–234, 1961.

[5] X. Hou, J. Harel, and C. Koch, "Image signature: Highlighting sparse salient regions," *IEEE TPAMI*, vol. 34, no. 1, pp. 194–201, 2012.

[6] S. Sangwine and T. Ell, "Colour image filters based on hypercomplex convolution," *IEEE Proc. Vision, Image and Signal Processing*, 2000.

[7] C. Guo, Q. Ma, and L. Zhang, "Spatio-temporal saliency detection using phase spectrum of quaternion fourier transform," in *CVPR*, 2008.

[8] C. Guo and L. Zhang, "A novel multiresolution spatiotemporal saliency detection model and its applications in image and video compression," *IEEE Trans. Image Process.*, vol. 19, pp. 185–198, 2010.

[9] B. Schauerte and R. Stiefelhagen, "Quaternion-based spectral saliency detection for eye fixation prediction," in *ECCV*, 2012.

[10] A. Borji, D. N. Sihite, and L. Itti, "Quantitative analysis of human-model agreement in visual saliency modeling: A comparative study," *IEEE Trans. Image Process.*, vol. 22, no. 1, pp. 55–69, 2013.

[11] D. Parkhurst, K. Law, and E. Niebur, "Modeling the role of salience in the allocation of overt visual attention," *Vision Research*, vol. 42, no. 1, pp. 107–123, 2002.

[12] L. Itti, C. Koch, and E. Niebur, "A model of saliency-based visual attention for rapid scene analysis," *IEEE TPAMI*, vol. 20, no. 11, pp. 1254–1259, 1998.

[13] J. Harel, C. Koch, and P. Perona, "Graph-based visual saliency," in *NIPS*, 2007.

[14] X. Hou and L. Zhang, "Saliency detection: A spectral residual approach," in *CVPR*, 2007.

[15] R. Achanta, S. Hemami, F. Estrada, and S. Süsstrunk, "Frequency-tuned Salient Region Detection," in *CVPR*, 2009.

[16] S. Lu and J.-H. Lim, "Saliency modeling from image histograms," in *ECCV*. 2012.

[17] A. R. Gillespie, A. B. Kahle, and R. E. Walker, "Color enhancement of highly correlated images. ii. channel ratio and chromaticity transformation techniques," *Remote Sensing of Environment*, vol. 22, pp. 343–365, 1987.

[18] E. Reinhard and T. Pouli, "Colour spaces for colour transfer," in *Computational Color Imaging*, vol. 6626 of *Lecture Notes in Computer Science*, pp. 1–15. 2011.

[19] A. J. Bell and T. J. Sejnowski, "The independent components of scenes are edge filters," *Vision Research*, vol. 37, no. 23, pp. 3327–3338, 1997.

[20] M. Brown, S. Susstrunk, and P. Fua, "Spatio-chromatic decorrelation by shift-invariant filtering," in *CVPR Workshop*, 2011.

[21] L. Duan, C. Wu, J. Miao, L. Qing, and Y. Fu, "Visual saliency detection by spatially weighted dissimilarity," in *CVPR*, 2011.

[22] J. Zhou, Z. Jin, and J. Yang, "Multiscale saliency detection using principle component analysis," in *Int. Joint Conf. on Neural Networks*, 2012, pp. 1–6.

[23] P.-H. Wu, C.-C. Chen, J.-J. Ding, C.-Y. Hsu, and Y.-W. Huang, "Salient region detection improved by principle component analysis and boundary information," *IEEE Trans. Image Process.*, vol. 22, no. 9, pp. 3614–3624, 2013.

[24] W. Luo, H. Li, G. Liu, and K. N. Ngan, "Global salient information maximization for saliency detection," *Signal Processing: Image Communication*, vol. 27, 2012.

[25] N. Bruce and J. Tsotsos, "Saliency, attention, and visual search: An information theoretic approach," *Journal of Vision*, vol. 9, no. 3, pp. 1–24, 2009.

[26] T. Judd, K. Ehinger, F. Durand, and A. Torralba, "Learning to predict where humans look," in *ICCV*, 2009.

[27] G. Kootstra, A. Nederveen, and B. de Boer, "Paying attention to symmetry," in *BMVC*, 2008.

[28] N. Riche, M. Duvinage, M. Mancas, B. Gosselin, and T. Dutoit, "Saliency and human fixations: State-of-the-art and study of comparison metrics," in *ICCV*, 2013.

[29] T. Jost, N. Ouerhani, R. von Wartburg, R. Mäuri, and H. Häugli, "Assessing the contribution of color in visual attention," *CVIU*, vol. 100, pp. 107–123, 2005.

[30] A. Olmos and F. A. A. Kingdom, "A biologically inspired algorithm for the recovery of shading and reflectance images," *Perception*, vol. 33, pp. 1463–1473, 2004.